22nd International Conference on Renewable Energies and Power Quality (ICREPQ'24)
Bilbao (Spain), 26th to 28th June 2024
Renewable Energy and Power Quality Journal (RE&PQJ)
ISSN 2172-038 X, Volume No.22, September 2024

Comprehensive Experimental Database and Model Fitting for Electric Arc Behavior in Aircraft Environments

S. Bogarra[1], M. Moreno-Eguilaz[2], J.A Ortega-Redondo[2] and J.-R. Riba[1]

[1] Department of Electrical Engineering
Universitat Politècnica de Catalunya
Campus of Terrassa, 08222 Terrassa (Spain)
Phone: +0034 937398365

[2] Department of Electronic Engineering
Universitat Politècnica de Catalunya
Campus of Terrassa, 08222 Terrassa (Spain)
Phone: +0034 937398365

Abstract. The More Electric Aircraft (MEA) paradigm advocates weight reduction by transitioning to electrical components, resulting in increased system voltage and higher arc fault risk. This paper presents a methodology for creating a database of nearly one thousand tests simulating parallel arc faults, using Andrea's arc model for accurate representation. Objectives include the creation of a robust experimental database and the use of a simplified model to analyze arcing behavior. The setup follows the UL 746A standard and considers various pressure and electrode separation conditions. The database includes 960 experiments with PVC and PTFE materials, and model fitting ensures accurate representation of arc currents and voltages. Error analysis shows consistent model performance across materials and highlights sensitivity to electrode spacing, pressure, and source voltage. The paper concludes with a clear 30% error threshold for model validity, enhancing the understanding of the applicability of Andrea's model under various experimental scenarios in aircraft environments.

Key words. More electric aircraft, electric arc modelling, low pressure, model fitting, experimental database.

1. Introduction

The More Electric Aircraft (MEA) involves replacing traditional hydraulic and mechanical components with their electrical counterparts, achieving weight reduction by increasing system voltage. As aircraft electrical power requirements increase and distribution system operating voltages rise, so does the likelihood of arc faults. Aircraft power distribution systems, including cables and busses, are exposed to harsh environmental conditions. Both cables and connectors are susceptible to damage, which is a major cause of arc faults. Understanding the behavior of arcing in aircraft is therefore increasingly important.
Conducting numerous arc tests with different electrode separation distances and pressure conditions is a labor-intensive and time-consuming task [1]. Furthermore, such information is often not available to the scientific community. Therefore, this paper outlines the methodology used to generate an extensive database of nearly one thousand tests that reproduce parallel arc faults.
Modeling an electric arc involves complicated equations and algorithms based on physical parameters, with parameter fitting from voltage and current measurements being a formidable challenge [2]-[6]. This difficulty is particularly significant given the often limited understanding of this complex phenomenon. As a result, a black-box model is often used to facilitate a quick yet sufficiently accurate analysis, especially in cases where the intricate nature of the phenomenon is not well understood [7]-[11]. Nevertheless, a simplified model can be sufficiently accurate in elucidating the behavior of the arc [12]-[13].
Most traditional arc models, commonly used as black box models, are based on two basic frameworks: the Cassie arc model and the Mayr arc model [14]-[15]. These models are based on experimentally unverified assumptions [16]. A power-based model with a significant number of parameters can be used to model the arc [17]. Fitting these models to experimental reality is challenging, and in particular, they lack the ability to reproduce arc fault scenarios within aircraft power systems. Traditional arc models fall short in simulating such scenarios. However, the arc model proposed by Andrea et al. stands out because it accurately captures these specific scenarios [18]-[19]. Therefore, Andrea's arc model was selected for its ability to accurately simulate the arc impedance and reproduce the desired scenarios.
The objectives of this article are twofold: first, to establish a comprehensive database of hundreds of tests conducted under varying conditions of pressure and electrode separation; and second, to employ a simple model that provides a robust fit in a significant number of cases within the aforementioned test database.
This paper is divided into four main sections: a detailed presentation of the arc model used in Section 2. Section 3 details the experimental setup, while Section 4 describes

the database obtained. Section 5 fits the arc model and determines the range of experimental conditions where the model is accurate enough. Finally, Section 6 highlights the conclusions of the work.

2. Electric Arc Modelling

The analysis of arcing faults in aircraft electrical systems is a significant challenge that requires in-depth study supported by an extensive database of arc signals [1]. This paper outlines the methodology used to conduct nearly a thousand tests, focusing on the analysis of arc voltages and currents using Andrea's arc model. The mathematical model described in reference [12] describes the dynamics of electric arcs in power circuits. A notable advantage is that the arc is treated as a circuit component, which facilitates its simulation by transient software such as MATLAB-Simulink.

Modern aircraft use three primary insulation systems: PI, XL-ETFE and PTFE/PI composite insulation. Although PVC has been used in some applications, its use is discouraged due to concerns over ageing issues. It is worth noting that PI insulation, although widely used, has a lower resistance to arc tracking. Therefore, in scenarios where arc tracking is a potential hazard, PI insulation should be avoided [22], [23].

Specifically, PTFE and PVC were used in the tests conducted. Features such as gap spacing or variations in electrode material and geometry can also contribute to significant differences in arc behavior. Andrea's model was used to match the arc scenarios described in the UL 746A standard [20]-[21]. This standard includes a section that addresses the resistance to ignition of high voltage arcs in polymeric materials under dry tracking conditions. In [18], Andrea's model was presented, emphasizing its ease of fitting to real cases, covering both arc ignition and extinction. The study compared experimental arc measurements with simulations for carbonized path ignition and classical Mayr-type models. The results indicate that the proposed model provides a superior description of arc behavior in circuits compared to the Mayr-type model. Given the proximity of our waveforms to those presented by the authors in the case of carbonized path ignition, we selected this model to simulate the tests in our current paper. Reference [19] uses Andrea's arc model to simulate arc faults in aircraft and to optimize the placement of arc fault protection.

The arc is conceptualized as a circuit component that establishes a relationship between arc current and arc voltage. This approach underlies the behavioral model outlined in [18] for describing electric arcs in power circuits.

The static relationship between arc current and voltage is defined by the following equation:

$$V_{arc} = F(I_{arc}) = \frac{\alpha R_C I_{arc}}{\arctan(\beta I_{arc}) I_{arc} R_C + \alpha} \qquad (1)$$

where V_{arc} and I_{arc} are the arc voltage and the arc current, R_C is the resistance corresponding to the resistive part of the static characteristic of the electric arc [12]. The parameter α can be initially fitted by measuring the limit voltage when the current goes to infinity using the following equation:

$$\alpha = \pm\frac{\pi}{2}\left(\lim_{I_{arc}\to\pm\infty} V_{arc}\right) \qquad (2)$$

The parameter β can be initially fitted by measuring the current I_{Text} corresponding to the maximum arc voltage using the following equation:

$$\beta^2\left(\alpha {I_{Text}}^2\right) - \beta\left(R_C {I_{Text}}^2\right) + \alpha = 0 \qquad (3)$$

In dynamic scenarios, where the arc time constant, τ, is non-negligible compared to the circuit time constant, the relationship between arc voltage and current is expressed as follows [18]:

$$V_{arc}(t) + \tau\frac{dV_{arc}(t)}{dt} = F\left(I_{arc}(t) + \tau\frac{dI_{arc}(t)}{dt}\right) \qquad (4)$$

where F is the static arc function shown in (1).

3. Experimental Setup

This paper investigates the behavior of an electric arc between two electrodes as a function of distance and pressure in the range of 100-10 kPa, corresponding to sea level and 16,000 m altitude, respectively, according to Standard Atmosphere [24] to ensure compatibility with aircraft environments. The test setup adhered to UL 746A [21], which includes a section on dry tracking high voltage arc resistance for polymeric materials. This test evaluates the ability of the material's surface to resist ignition or form a visible carbonized path when exposed to a low-current, high-voltage arc. The setup used 303 stainless steel rod electrodes with an outer diameter of 3.2 mm and a length of approximately 102 mm, with the tips machined to a symmetrical conical point at a 30° angle in accordance with UL 746A recommendations. These metal electrodes are spaced at an adjustable distance [1mm-12mm] above an insulator specimen, as shown in Fig. 1. In this work, two materials are tested for the specimen: PVC and PTFE.

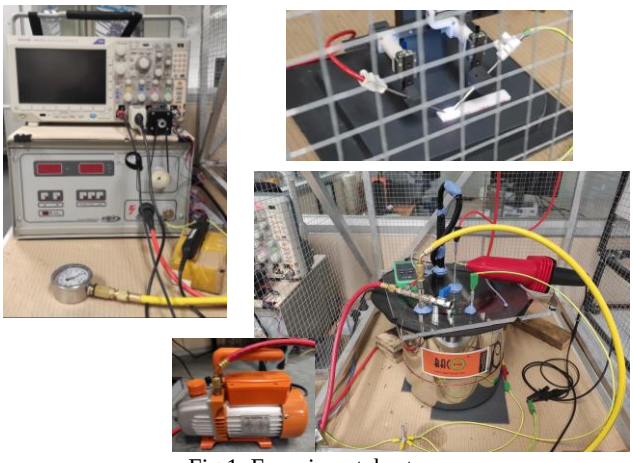

Fig.1. Experimental setup

The experiments were conducted in a stainless steel pressurized chamber (130 mm diameter and 375 mm

height). The low-pressure chamber allows the internal pressure to be varied within a range of 10-100 kPa, covering the pressure level of most commercial aircraft. A BA-1 vacuum pump (Bacoeng, Suzhou, China) was used to regulate the pressure inside the low-pressure chamber.
For safety reasons, i.e. to protect both the operators and the electrical and electronic equipment from unwanted contact with the high voltage supply, the low-pressure chamber is located inside a box-like metal Faraday cage connected to ground, as shown in Fig. 1. An adjustable voltage source (Tecnolab RD-6 10 kVRMS, 50 mARMS, 600 VA max output power) was used to supply the high voltage to the test specimens of different materials. The voltage of the electric arc generated between the electrodes of the experimental setup was measured with a TT-HVP40 high voltage probe (Testec Elekronik, Dreieich, Hessen, Germany). The current of the generated arc was measured with a high-frequency current probe (Tektronix TCP0030A, bandwidth 120 MHz, 1% DC gain error). A Tektronix MDO3024 oscilloscope (four channels, 200 MHz, 2.5 Gsamples/s) was used to record the voltage and current of the electric arc obtained under various low pressure conditions.

4. Database

Electric arc behavior under various experimental conditions has been extensively studied due to its importance in numerous aerospace applications. In this study, we present a comprehensive experimental database aimed at elucidating the effects of pressure, electrode spacing, and material composition on electric arc characteristics. The experimental setup included a wide range of conditions, including pressure levels ranging from 0.1 bar to 1 bar, electrode distances ranging from 1 mm to 12 mm, and two different materials: PVC and PTFE.
Each experimental condition was carefully studied with four repetitions, resulting in a total of 960 experiments. The pressure was increased in steps of 0.1 bar, while the electrode distance was varied at 1 mm intervals. During each experiment, the arc was maintained for approximately 4-5 periods at a frequency of 50 Hz.
The database consists of 960 individual files, each of which stores the arc voltage and current data (see Fig. 2) along with their corresponding scales. In addition, each experiment is accompanied by a Microsoft Excel file containing key environmental parameters such as temperature, relative humidity, pressure, and electrode spacing. This comprehensive approach ensures that the influence of environmental factors on arc behavior can be thoroughly analyzed.
In addition, the database includes photographic documentation of specimens before and after each test, allowing visual inspection of any physical changes induced by the electric arc. This inclusion provides researchers with valuable insight into the morphological changes and damage mechanisms associated with different experimental conditions.

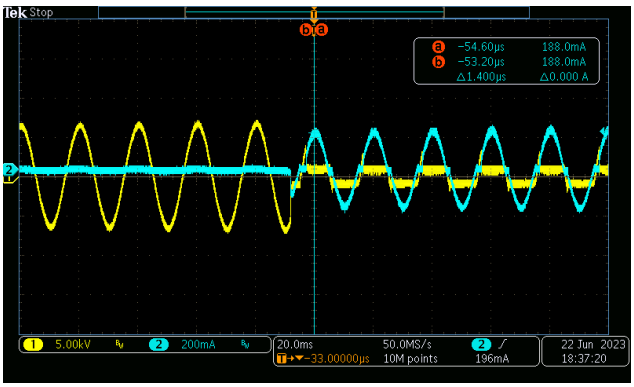

Fig.2. Experimental voltage and current waveforms of an electric arc

5. Model Fitting

This section provides a detailed description of the parameter fitting process and error analysis applied to the mathematical modeling of arc currents and voltages.

A. Model parameter fitting
The first step is to isolate the stable positive half-cycles identified in all the experiments documented in the database.

Subsequently, the parameters α, β, R_C and τ of Andrea's model [12], [18] are fitted individually for each isolated half-cycle. This fitting process uses an optimization technique aimed at minimizing the error as defined in (5):

$$\varepsilon_{opt} = \frac{1}{2} \cdot \mathrm{RMS}\left(\varepsilon_{V_{opt}}\right) + \frac{1}{2} \cdot \mathrm{RMS}\left(\varepsilon_{I_{opt}}\right) \quad (5)$$

where:

$$\mathrm{RMS}\left(\varepsilon_{V_{opt}}\right) = \frac{1}{N}\sqrt{\sum \left|\frac{V_{data} - V_{opt}}{\max\left(V_{data}\right)}\right|^2} \quad (6)$$

$$\mathrm{RMS}\left(\varepsilon_{I_{opt}}\right) = \frac{1}{N}\sqrt{\sum \left|\frac{I_{data} - I_{opt}}{\max\left(I_{data}\right)}\right|^2} \quad (7)$$

where:
I_{opt} and V_{opt} are the current and voltage of the electric arc, respectively, reconstructed by using the mathematical model with the optimal parameters. I_{data} and V_{data} are the experimental current and voltage of the electric arc, respectively, and N is the number of samples of I_{data} and V_{data}.
The resulting parameters α, β, R_c, and τ ensure that the model closely matches the experimental data. This iterative optimization minimizes the differences between the measured (I_{data}, V_{data}) and modeled (I_{opt}, V_{opt}) signals for current and voltage, respectively.
As an example, Fig. 3 shows the results of the fitting process under various experimental conditions for arc voltage and current in a half cycle. The results demonstrate the ability of the model to accurately represent arc currents and voltages. The fits are not only accurate, but also consistent across different experimental scenarios.

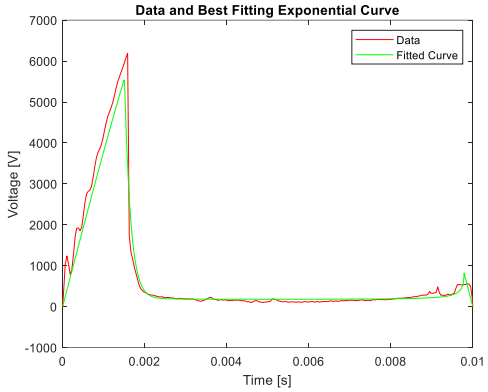

(a) Experimental and fitted voltage for PVC d = 12 mm, p = 1 bar

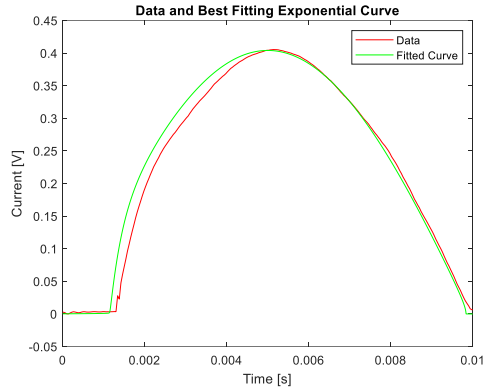

(b) Experimental and fitted current for PVC d = 12 mm, p = 1 bar

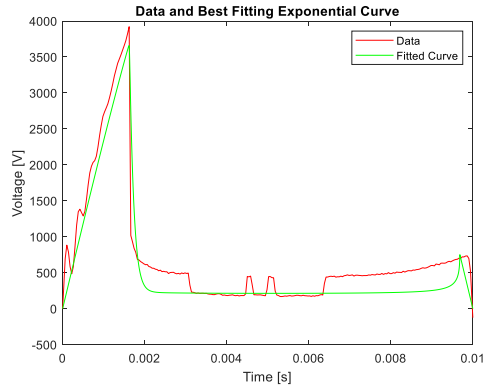

(c) Experimental and fitted voltage for PTFE d = 5 mm, p = 0.8 bar

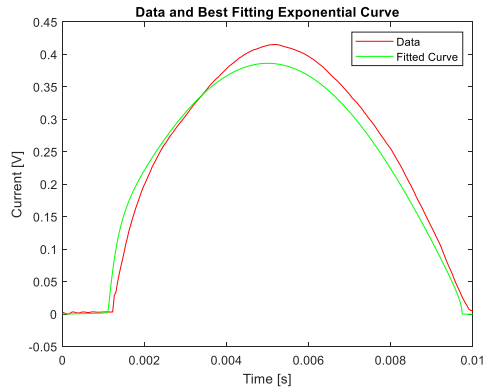

(d) Experimental and fitted current for PTFE d = 5 mm, p = 0.8 bar

Fig.3. Comparison of experimental and fitted electric arc voltage and current waveforms for different experimental conditions

The visual analysis shows that the model fits are robust and independent of the material used in the experiments. This highlights the generalizability of the Andrea's model, making it a reliable tool for predicting arc behavior across different materials and experimental conditions.

B. Model error analysis

Fig. 4 shows histograms detailing the distribution of errors obtained during the fitting of each individual half-cycle for both PVC and PTFE materials. It is noteworthy that the histograms show a consistent error, as defined in (5), distributed around 20%. This uniformity in the error distribution suggests that Andrea's model exhibits robust performance, providing reliable fits across different materials.

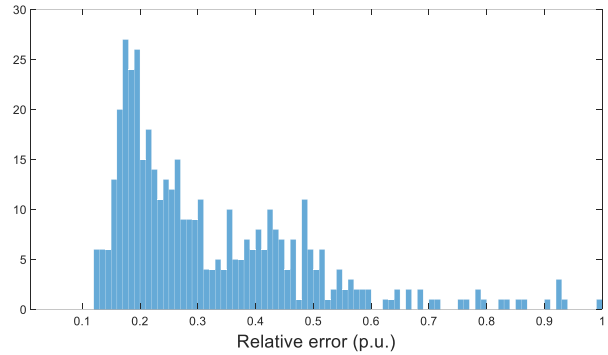

(a) Fitting error histogram for PVC

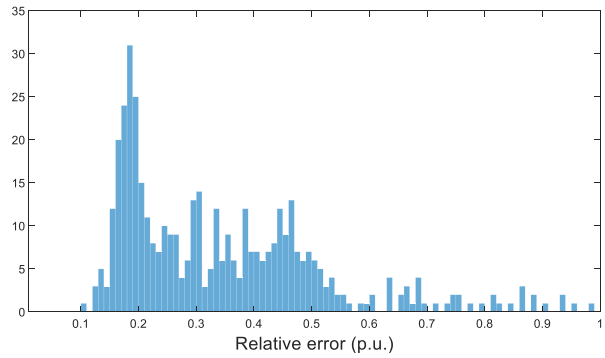

(b) Fitting error histogram for PTFE

Fig.4. Model error distribution for PVC and PTFE materials

To further investigate the relationship between modeling errors and experimental parameters, Fig. 5 is introduced. This figure shows the modeling error for each half-cycle plotted versus the source voltage V_{max}. The long-term trend of the error, represented by the blue line, shows a decreasing error with increasing V_{max} for both PVC and PTFE materials. This observation provides valuable insight into the sensitivity of the model to changes in source voltage and provides a basis for understanding how experimental conditions affect the accuracy of model predictions.

Fig. 6 goes deeper into the analysis by presenting a heat map illustrating the relationship between V_{max}, electrode distance, and pressure for both PVC and PTFE experiments.

The observations in Fig. 6, coupled with the trend shown in Fig. 5, lead to a compelling conclusion: experiments with larger electrode spacings and higher pressures result

in smaller modeling errors compared to those with smaller electrode spacings and lower pressures.

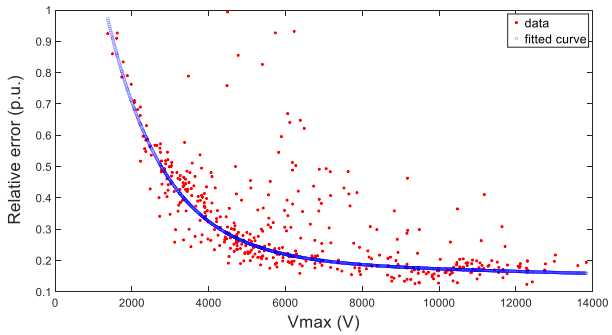

(a) PVC

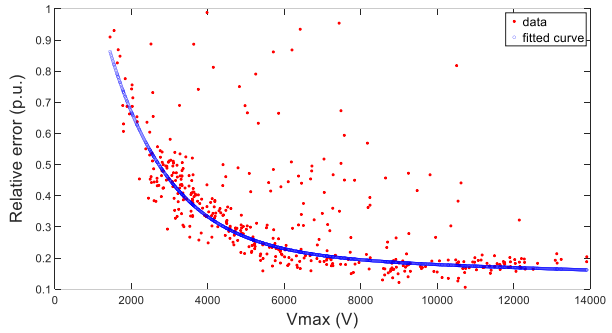

(b) PTFE

Fig.5. Modeling error versus the source voltage V_{max} for different materials

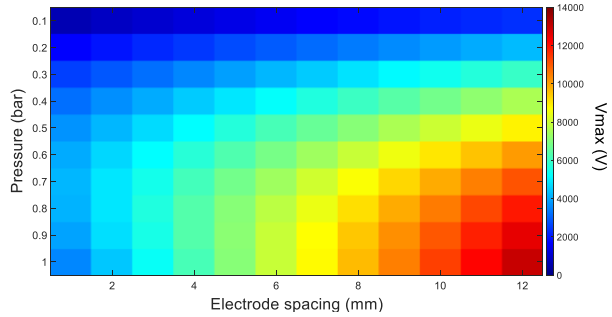

(a) PVC

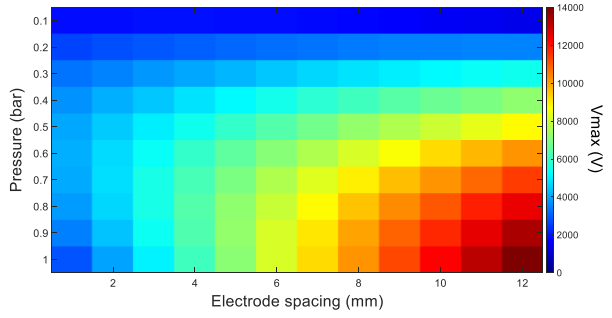

(b) PTFE

Fig.6. Heat maps of V_{max} versus electrode distance and pressure for different materials

By setting a 30% error threshold for model validity, Fig. 7 is introduced to provide a clear visualization of the model's valid experimental condition space (light-colored region). This figure encapsulates the regions where the proposed model is considered reliable, effectively establishing a robust boundary for the applicability of the model under varying experimental conditions.

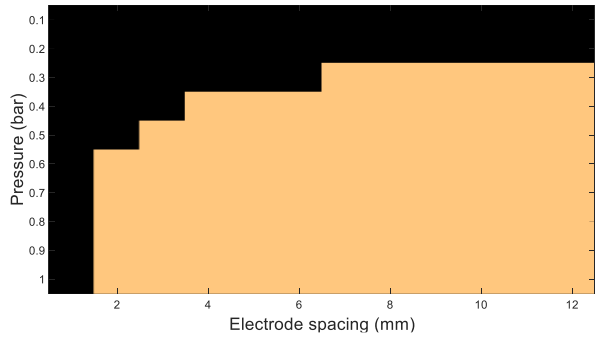

(a) PVC

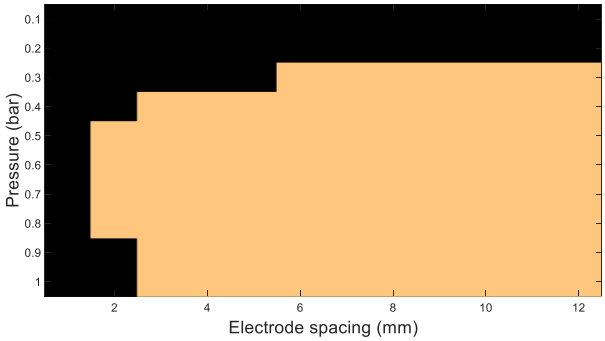

(b) PTFE

Fig.7. Maps of experimental conditions for reliable modelling for different materials

6. Conclusions

In conclusion, the developed experimental database serves as a valuable resource for studying electric arc behavior under various conditions. Its comprehensive nature, including various experimental parameters and accompanying environmental data, facilitates in-depth analyses and contributes to a deeper understanding of electric arc phenomena in practical applications.

The process of adjusting the parameters of Andrea's model ensures a versatile and accurate representation of electric arcs, demonstrating the model's ability to capture the complexities of both voltage and current waveforms.

The subsequent analysis of the fitting errors shows that the model performs consistently well across different materials. Exploration of the error dependence on experimental parameters sheds light on the intricate relationship between electrode distance, pressure, and source voltage, providing valuable insights for experimental design and interpretation.

The establishment of a 30% error threshold provides a clear criterion for model validity. This criterion, combined with the analyses presented in the paper, contributes to a comprehensive understanding of the applicability and reliability of the Andrea's model under different experimental scenarios.

Acknowledgement

This research was partially funded by Ministerio de Ciencia e Innovación de España, grant number PID2020-114240RB-I00 and by the Generalitat de Catalunya, grant

number 2021 SGR 00392. Special thanks to the Laboratori Comú d'Enginyeria Mecànica (LCEM) of the Universitat Politècnica de Catalunya for the design and manufacture of the mechanical prototype of this project.

References

[1] A. Chabert, P. Schweitzer, S. Weber and J. Andrea, "State-space simulation of electric arc faults", IEEE Transactions on Aerospace and Electronic Systems (2022), Vol. 58, no. 3, pp. 1650-1659.

[2] J. L. Zhang, J. D. Yan, A. B. Murphy, W. Hall and M. T. C. Fang, "Computational investigation of arc behavior in an auto-expansion circuit breaker contaminated by ablated nozzle vapor", IEEE Transactions on Plasma Science (2002), vol. 30, no. 2, pp. 706-719.

[3] C. L. Yao, H. C. Zhu, Z. H. Jiang and T. Pan, "Numerical analysis of fluid flow and heat transfer by means of a unified model in a direct current electric arc furnace", Steel Research International (2021), vol. 92, no. 6, pp. 2000664.

[4] Z. Liu, Y. Li and Y. Su, "Simulation and analysis of heat transfer and fluid flow characteristics of arc plasma in longitudinal magnetic field-tungsten inert gas hybrid welding", International Journal of Advanced Manufacturing Technology (2018), vol. 98, pp. 2015-2030.

[5] J. D. Hernández, L. Onofri and S. Engell, "Numerical estimation of the geometry and temperature of an alternating current steelmaking electric arc", Steel Research International (2021), vol. 92, no 3, pp. 2000386.

[6] F. Jiang, X. Gao, B. Xu, G. Zhang, C. Fan, S. Tashiro and S. Chen, "Numerical analysis of arc physics and energy transfer under circumferential gas constraint effect", International Journal of Heat and Mass Transfer (2024), vol. 221, pp. 125082.

[7] A. Khakpour, S. Franke, S. Gortschakow, D. Uhrlandt, R. Methling and K.D. Weltmann, "An improved arc model based on the arc diameter", IEEE Transactions on Power Delivery (2016), vol. 31, no. 3, pp. 1335-1341.

[8] A. Khakpour, D. Uhrlandt, R. Methling, S. Gortschakow, S. Franke, M.T. Imani and K.D. Weltmann, "Impact of temperature changing on voltage and power of an electric arc", Electric Power Systems Research (2017), vol. 143, pp. 73-83.

[9] A. Balestrero, L. Ghezzi, M. Popov, G. Tribulato and L. van der Sluis, "Black box modeling of low-voltage circuit breakers", IEEE Transactions on Power Delivery (2010), vol. 25, no. 4, pp. 2481-2488.

[10] J. He, K. Wang and J. Li, "Application of an improved Mayr-type arc model in pyro-breakers utilized in superconducting fusion facilities", Energies (2021), vol. 14, no. 14, pp. 4383.

[11] K.H. Park, H.Y. Lee, M. Asif and B.W. Lee, "Parameter identification of dc black-box arc model using non-linear least squares", The Journal of Engineering (2019), vol. 2019, no. 16, pp. 2202-2206.

[12] J. Andrea, P. Besdel, O. Zirn and M. Bournat, "The electric arc as a circuit component", IECON 2015-41st Annual Conference of the IEEE Industrial Electronics Society (2015), pp. 003027-003034.

[13] J. Andrea, P. Schweitzer and J.M. Martel, "Arc fault model of conductance. Application to the UL1699 tests modelling", IEEE 57th Holm Conference on Electrical Contacts (2011), pp. 1-6.

[14] U. Habedank, "Application of a new arc model for the evaluation of short-circuit breaking tests", IEEE Transactions on Power Delivery (1993), vol. 8, no. 4, pp. 1921-1925.

[15] S. Golestani and H. Samet, "Generalised Cassie–Mayr electric arc furnace models", IET Generation, Transmission & Distribution (2016), vol. 10, no. 13, pp. 3364-3373.

[16] M. Walter and C. Franck, "Improved method for direct black-box arc parameter determination and model validation", IEEE Transactions on Power Delivery (2014), vol. 29, no. 2, pp. 580-588.

[17] A. Khakpour, S. Franke, D. Uhrlandt, S. Gortschakow and R. Methling, "Electrical arc model based on physical parameters and power calculation", IEEE Transactions on Plasma Science (2015), vol. 43, no. 8, pp. 2721-2729.

[18] J. Andrea, M. Bournat, R. Landfried, P. Testé, S. Weber, and P. Schweitzer, "Model of an electric arc for circuit analysis", Proc. 28th Int. Conf. Electr. Contacts (2016), pp. 361–366.

[19] J. Andrea, M. Buffo, E. Guillard, R. Landfried, R. Boukadoum and P. Teste, "Arcing fault in aircraft distribution network", Proc. IEEE Holm Conf. Elect. Contacts (2017), pp. 317–324.

[20] J.-R. Riba, M. Moreno-Eguilaz and S. Bogarra, "Tracking resistance in polymeric insulation materials for high-voltage electrical mobility applications evaluated by existing test methods: identified research needs", Polymers (2023), vol. 15, no.18, pp. 3717.

[21] UL 746A, "Polymeric Materials—Short Term Property Evaluations", UL: Northbrook, IL, USA (2012), pp. 1–48.

[22] J.-R. Riba, M. Moreno-Eguilaz and J.A. Ortega, "Arc fault protections for aeronautic applications: a review identifying the effects, detection methods, current progress, limitations, future challenges, and research needs", IEEE Transactions on Instrumentation and Measurement (2022), vol. 71, pp. 1-14.

[23] J.-R. Riba, Á. Gómez-Pau, M. Moreno-Eguilaz and S. Bogarra, "Arc tracking control in insulation systems for aeronautic applications: Challenges, opportunities, and research needs", Sensors (2020), vol. 20, no. 6, pp. 1654.

[24] ISO, "ISO 2533:1975 - Standard Atmosphere" (1975), pp. 1–11.